Post Processing Sparse and Instantaneous 2D Velocity Fields using Physics-Informed Neural Networks

Diego Di Carlo[1,*], Dominique Heitz[2], Thomas Corpetti[1]

1: Univ. de Rennes 2, LETG, CNRS, Rennes, France
2: INRAE, OPAALE, Rennes, France
*Corresponding author: diego.dicarlo89@gmail.com

Keywords: Physics-informed Neural Networks, Super resolution, Vector fields, PTV

ABSTRACT

This work tackles the problem of resolving high-resolution velocity fields from a set of sparse off-grid observations. This task is here addressed with deep neural network models trained to satisfy physics-based constraints in an unsupervised fashion. Finally, a sub-grid model is proposed to improve the accuracy and physical consistency of the super-resolved velocity fields of turbulent flows.

1. Introduction

Spatial reconstruction of physical velocity fields from sparse observation is still an open challenge with relevant applications in many research fields spanning from environmental science, physics simulations and measurements, medical images to computer graphics. Traditional super-resolution (SR) techniques, such as least-squared optimization or kernel-based interpolation, are typically easy to implement, but the output may not capture the physical nature of the problem. Besides, prior knowledge about the physical laws sometimes leads to intractable problems or is tricky to implement.

Recently deep learning (DL) has been used to address SR problems with exceptional and striking results, especially in image processing and computer vision. In particular, Convolutional Neural Networks (CNN) show impressive results on image-like data. However, such approaches are counterbalanced by requiring that the input data be organized in a regular grid, preventing training and evaluating points on distributed irregular or sparse mesh. In addition, as common to data-driven approaches, the performances depend on the availability of training datasets, and accuracy may drop in unseen test conditions.

Despite these drawbacks, the modularity of the neural network architectures and training loss functions lend DL models to embed custom prior knowledge. In particular, the recently proposed physics-informed neural networks (PINNs) show the possibility of constraining the output of a

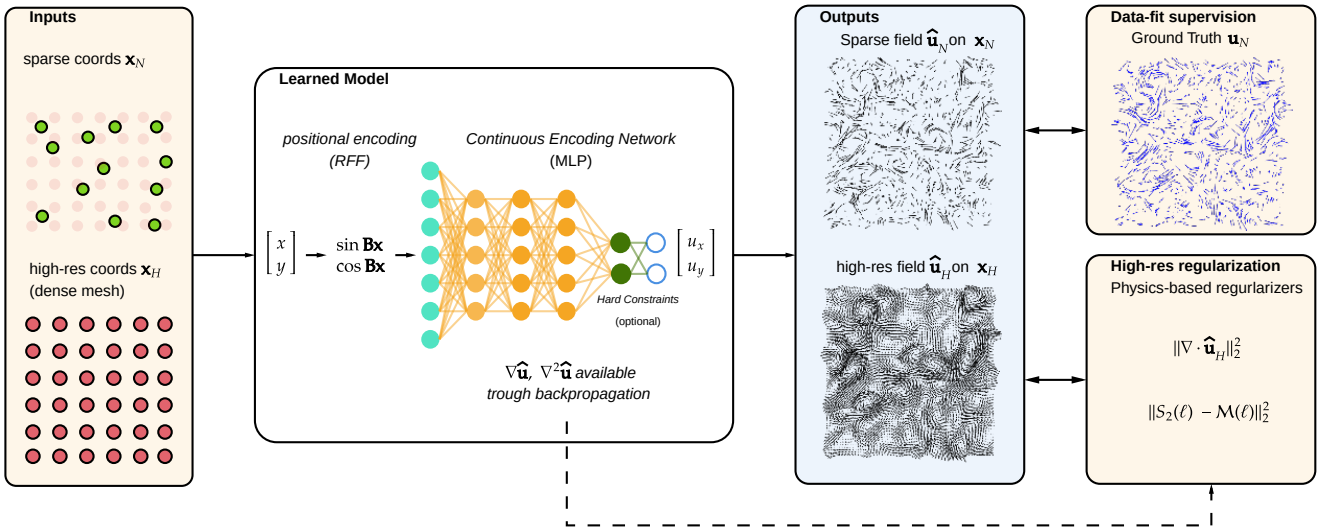

Figure 1. Pipeline of the the proposed approach for super-resolution of sparse and instantaneous 2D velocity fields. The MLP network takes coordinates as inputs and estimates associated velocities. Its optimization on grids enables to impose spatial constraints

NN to satisfy a physical model, often described by partial differential equations (PDEs), leading to more scientifically valid and robust predictions (Kashinath et al., 2021; Vinuesa & Brunton, 2021).

This work propose a novel framework based on Physics-informed Neural Networks to reconstruct instantaneous and sparse 2D velocity fields. In particular:

- We demonstrate how physics-informed neural networks can be used as post-processing tool to reconstruct instantaneous velocity fields from sparse measurement: once trained to reconstruct sparse data, the model can evaluate the vector field on a denser regular grid.
- We propose an unsupervised self-similarity constraint derived from Kolmogorov's theory for turbulent flows that aim to resolve the highest resolution scales properly.
- Experimental results showed the possibility of super-resolving typical Particle Tracking Velocimetry (PTV) measurements, starting from 0.03 vector per pixel stochastically distributed and providing up to 1 vector per pixel on a regular grid with a mean angular error smaller than 8 degrees.

Finally, the python code to reproduce the results presented in this work are publicly available*.

2. Related Works

Other then standard bi-cubic interpolation-based methods (Keys, 1981), traditional approaches for vector field reconstruction rely on feature sparsity-based techniques (Yang et al., 2010; Callaham et

*https://github.com/Chutlhu/TurboSuperResultion/tree/lxlaser22

al., 2018) , image deconvolution (Zille et al., 2016), kernel interpolation using divergence-free (McNally, 2011; Macêdo & Castro, 2010; Busch et al., 2013; Gunes & Rist, 2007) or wavelet-based approaches (T. Kim et al., 2008; Deriaz & Perrier, 2006). These methods are commonly used in commercial softwares and are supported by literature that spans decades. However, they suffer from known numerical instability, computational complexity, and the implementation of arbitrary prior knowledge is often challenging. Recently, several DL approaches have been applied for reconstructing velocity fields of turbulent flows. Most of the state-of-the-art rely on CNN-based models, e.g., (Lee et al., 2017; H. Kim et al., 2021; Fukami et al., 2019; Cai et al., 2019).

To embed governing physical laws, some works rely on *soft* constraints, i.e., adding physical properties as divergence-free (Bode et al., 2021) or PDEs residuals based on the Navier-Stokes equations (Esmaeilzadeh et al., 2020; C. Wang et al., 2020) in the objective function. Other studies rely on *hard* constraints where the physical rules are respected by construction. For instance, in (B. Kim et al., 2019; Mohan et al., 2020), the authors propose a CNN-based architecture that outputs the scalar potential from which the velocity field is retrieved by taking the curl of such quantity, guaranteeing divergence-free. Differently, the work in (R. Wang et al., 2020) proposes a multi-scale U-Net architecture that processes the flow at different spatio-temporal scales, filtered according to theoretical models. The main disadvantage of these approaches is the need of high-resolution (HR) data for supervising the training. Interestingly, the work in (Gao et al., 2021) proposes to use a data-assimilation framework for unsupervised training.

Specific to static vector fields, the works in (Bar-Sinai et al., 2019; Kochkov et al., 2021) propose to use DL together with a stencil-based interpolation scheme, while in (Li et al., 2020) a new resolution-invariant layer, dubbed Fourier Neural Operator, is introduced. Despite the outstanding results, these architectures do not generalize directly to grid-free test points. To overcome the limit, the work in (Esmaeilzadeh et al., 2020) extend the CNN-based approach to query grid-free data at test time, yet requiring LR data structured on a uniform grid.

In their original version, Physics-informed Neural Network (PINNs) (Raissi et al., 2019) are Multi-Layer Perceptor (MLP)-based models that aim to approximate the solution to PDEs by minimizing their residual error. The core intuition behind PINNs is that the back-propagation algorithm can be used to access derivatives with respect to inputs directly. Several works have already applied PINNs to turbulent flows with success (Bottero et al., 2020; Jin et al., 2021; Lu et al., 2021). Unfortunately, PINNs suffer from issues that prevent 1) encoding accurately high-frequency details, and 2) guaranteeing the right minimization of all the loss terms (S. Wang et al., 2021). To overcome the former, the authors of (Tancik et al., 2020) propose to encode the input with Random Fourier Features (RFF) able to capture more variability in frequencies. The latter issue can be addressed by using techniques for multi-task learning (S. Wang et al., 2021).

The significant benefit of PINNs are two-folds. First, MLPs can be viewed as a kernel-based interpolation model that, once trained on Low Resolution (LR) data, can interpolate the learned function on an denser input mesh (Jacot et al., 2018). Second, MLP can process input data points independently, without any requirement on their spatial structure. However, this may lead to

biased gradient estimation, distorting the results.

3. Method

3.1. Neural networks for divergence-free super-resolution

This work considers an instantaneous divergence-free, isotropic and homogeneous turbulent flow described by Navier-Stokes equations. Let $\mathbf{u}_H \in \mathbb{R}^{H\times H}$ be a high-resolution velocity field defined over the grid $\mathbf{x}_H \in \mathbb{R}^{H\times H}$. Here H corresponds to the highest possible resolution scale that entirely resolves the target flow. Let $\mathbf{x}_N, \mathbf{u}_N \in \mathbb{R}^{N\times 2}$ with $N \ll H^2$ be the observed *sparse* and *off-grid* coordinates and velocity vectors, respectively. Note that, since $\mathbf{u}_N$ and $\mathbf{x}_N$ are not necessarily on a grid, it is more convenient to define them as of N coordinates in $\mathbb{R}^2$. Finally, let $\mathbf{u}_L \in \mathbb{R}^{L\times L}$ with $L \ll H$ a low-resolution (LR) velocity vectors defined over the uniform coarse grid $\mathbf{x}_L \in \mathbb{R}^{L\times L}$. L and N are chose so that $\mathbf{u}_L$ and $\mathbf{u}_N$ (risp. $\mathbf{x}_L$ and $\mathbf{x}_N$) have the comparable density in terms of particle per pixel.

Following the RFF-based PINNs framework presented in (S. Wang et al., 2021), we use an MLP to learn the mapping between sparse coordinates $\mathbf{x}_N$, encoded into RFF (Tancik et al., 2020), and the sparse velocity components $\mathbf{u}_N$. A schematic overview of the network is depicted in Figure 1. Such model is trained by minimizing the mean-squared loss function between the given LR velocity field and the model prediction:

$$\mathcal{L}_{\text{rec}} = \frac{1}{L^2}\sum_{i,j} \|\mathbf{u}_N[i,j] - \hat{\mathbf{u}}_N[i,j]\|_2^2, \tag{1}$$

where $\hat{\mathbf{u}}_N[i,j] = \texttt{MLP}(\mathbf{x}_N[i,j])$ is the estimated velocity on indices i,j, hereafter dropped for sake of clarity.

Under the theory Neural Tangent Kernel (Jacot et al., 2018), MLPs can be viewed as a kernel-based interpolation model that, once trained on LR data, can interpolate the learned function on a denser input mesh. Once trained on the sparse data $(\mathbf{x}_N, \mathbf{u}_N)$, this model can directly evaluate velocity on arbitrary input mesh, e.g., $\mathbf{x}_L$ or $\mathbf{x}_H$.

In order to enforce physical consistency to the output of the neural network, one can add constraint derived from physical laws and models. Divergence-free soft constraints (Bode et al., 2021) can be added to (1), yielding a loss $\mathcal{L}_{\text{tot}}$ defined as:

$$\mathcal{L}_{\text{tot}} = \mathcal{L}_{\text{rec}} + \lambda_{\text{df}}\mathcal{L}_{\text{df}}, \tag{2}$$

$$\mathcal{L}_{\text{df}} = \|\nabla \cdot \mathbf{u}_N\|_2^2, \tag{3}$$

where λ_{df} is a scalar parameter that can be tuned manually or automatically (S. Wang et al., 2021). Alternatively, one can impose the divergence-free constraint as a hard constraint by predicting the

scalar potential $\Psi_{\mathbf{u}_N}$ and then taking its curl $\mathbf{u}_N = \nabla \times \Psi_{\mathbf{u}_N}$ (B. Kim et al., 2019; Mohan et al., 2020; Hendriks et al., 2020; Beucler et al., 2021), yielding by construction a divergence free velocity $\mathbf{u}_N$.

Note that the ∇ operation can be simply achieve by computing the derivatives of the model's output with respect to the inputs using automatic differentiation directly available in deep learning libraries.

3.2. Sub-scale regularization

Despite interesting results, hard constraints lead to high-frequency artifacts and inconsistent estimation of the gradient of the target function. In order to avoid such artifacts and increase the accuracy, we propose to use one novel regularization term by exploiting finer grid $\mathbf{x}_H$ constraints without requiring HR data $\mathbf{u}_H$. In fact, even though the high-resolution target data $\mathbf{u}_H$ are not available during train and validation, nothing prevents us from evaluating the physical consistency on $\mathbf{x}_H$ at training time. This can be extended to any resolution grid, such as $\mathbf{x}_L$.

The sub-grid self-similarity constraint (Héas et al., 2012) can be derived from Kolmogorov's theoretical works on turbulent flows. More precisely, homogeneity and isotropy at small scale can be translated as an invariance with respect to position $\mathbf{x}$ and direction $\mathbf{n}_\theta$. In particular, the statistical distribution of the velocity increments $\delta_u(\ell, \mathbf{x}, \theta) = [\mathbf{u}(\mathbf{x} + \ell\mathbf{n}_\theta) - \mathbf{u}(\mathbf{x})] \cdot \mathbf{n}_\theta$ at very low scale, i.e. below the elementary scale of the energy cascade, is driven by the following power law:

$$S_2(\ell) = \mathbb{E}_{\mathbf{x}} \left[\mathbb{E}_{\mathbf{n}_\theta} \left[|\delta_u(\ell, \mathbf{x}_H, \theta)|^2 \right] \right] \approx \gamma \ell^2, \tag{4}$$

where γ is a scale parameters of the flow that can be estimated from the LR data. In the literature $S_2(\ell)$ is known as the second-order *structure function* (Effinger & Grossmann, 1987). The formulation (4) is valid for $\ell < \eta$, where η is the Kolmogorov scale or the elementary scale of the energy cascade (in the following $\ell \in [0, 4]$ pixel wrt HR grid). Finally, the model (4) can translated into the soft constraint $\mathcal{L}_{\text{Sfun}}$ as

$$\mathcal{L}_{\text{Sfun}} = \frac{1}{2} \| S_2(\ell) - \gamma \ell^2 \|_2^2. \tag{5}$$

The resulting loss function features a weighted sum of these constraints forming a multi-task learning loss, that is

$$\mathcal{L}_{\text{tot}} = \mathcal{L}_{\text{rec}} + \lambda_{\text{df}} \mathcal{L}_{\text{df}} + \lambda_{\text{Sfun}} \mathcal{L}_{\text{Sfun}}. \tag{6}$$

4. Experimental results

To validate the proposed approach, we use a dataset of synthetic images sequences based on 2D turbulence obtained from direct numerical simulation (DNS) of the 2D and divergence-free Naiver-Stokes equation with a Reynolds number equal to 3000. The highest resolution of such images is

Hyper-parameter	Value
Batch size	256
Number of Random Fourier Features	512
Number of linear layers	5
Size of linear layers	256
Activation function	Tanh
Optimizer	Adam
Learning rate	5E-3
Weight decay	1E-4
λ_{div}	1E-3
λ_{sfun}	1E-2

Table 1. The configuration of hyper-parameter for the proposed model yielding the best performances.

256×256 pixel^2, corresponding to the lowest Kolmogorov scale for such flow. The experiments conducted in this research were carried out using the following Python libraries: Pytorch for deep learning and Scypy for signal processing. In terms of hardware, our experiments run on a GPU Quadro RTX 5000 with 16 GB of RAM.

Different models are evaluated by reconstruction error (i.e., root mean squared error between prediction and target) and angular error (in degree) on the reconstructed LR and HR vector fields for different hyper-parameters, such as network size, number of RFF, and different weights for the loss function, etc. Table 1 reports the configuration of hyper-parameters yielding the best performances considering different time-shots of the same flow.

The main results are showcased in Table 2 for an original sparse vector field simulating a PTV output obtained with 0.03 particle per pixel (ppp), hence providing 0.03 vector per pixel (vpp). Such field is synthetically built by randomly sampling at desired density the upsampled† ground-truth HR data. The models are evaluated for reconstructing a vector field on a uniform grid at different resolution: 64×64 corresponding at 0.25 vpp., 128×128 (0.5 vpp), and 256×256 (1 vpp). In addition, we will include the different terms of loss function (6) as a measure of fidelity of physical laws. Finally, we visually inspect the TKE spectrum and the reconstructed field.

We evaluated the proposed framework against classic bicubic interpolation, taken as baseline. We first observe that the simplest model RFFMLP outperforms the baseline, yielding angular error below 5°, demonstrating the effectiveness of neural networks models.

Secondly, we observe that the self-similarity regularization improves the models' performance in all the cases. In our view, this is a significant property since this term imposes the velocity field at small scales to follow physically motivated behaviour. In general, regarding the divergence-free constraints, the soft-constrain-based model seems to outperform the hard-constrained one in terms of the evaluation metrics, yielding an angular error of 10 times smaller. However, the divergence-free constraint is not guaranteed on the overall image as revealed by the value of the related residual ($\mathcal{L}_{\text{div}} \sim 10^{-2}$), while with hard-constraint is on the order of 10^{-11}. This issue seems to be due to inconsistency in estimating the high frequency of the solution learned by the neural

†Bicubic interpolation is used at the highest possible resolution.

	64×64 (0.25 vpp)		128×128 (0.5 vpp)		256×256 (1 vpp)	
	$\mathcal{L}_{\text{rec}}$	$\lambda_{\text{Sfun}}\mathcal{L}_{\text{sfun}}$	$\mathcal{L}_{\text{rec}}$	$\lambda_{\text{Sfun}}\mathcal{L}_{\text{sfun}}$	$\mathcal{L}_{\text{rec}}$	$\lambda_{\text{Sfun}}\mathcal{L}_{\text{sfun}}$
Bicubic	15.87° (2.83)	-	17.77° (3.23)	-	18.78° (3.31)	-
RFFMLP	4.87° (1.83e-2)	2.93° (0.62e-2)	4.77° (1.80e-2)	2.89° (0.61e-2)	4.78° (1.81e-2)	2.89° (0.62e-2)
soft-div RFFMLP	1.56° (0.18e-2)	**1.50° (0.14e-2)**	1.53° (0.17e-2)	**1.44° (0.13e-2)**	1.54° (0.18e-2)	**1.44° (0.13e-2)**
hard-div RFFMLP	12.43° (8.72e-2)	7.22° (3.16e-2)	11.93° (8.33e-2)	7.20° (3.16e-2)	11.96° (8.40e-2)	7.21° (3.16e-2)

Table 2. Comparison of reconstruction performances in terms of angular error and end point error (in parenthesis in pixel) for different resolution grid (the best results are in bold, vpp stands for vector per pixel). All the models are trained on sparse data with 0.03 vpp.

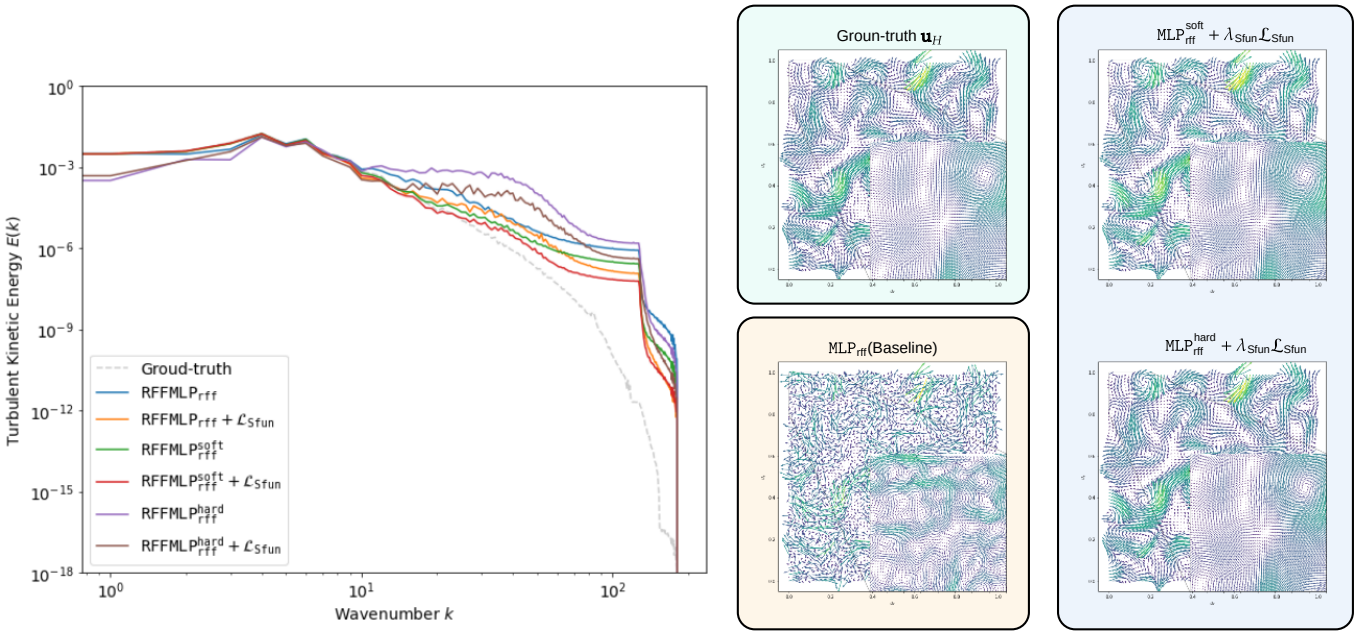

Figure 2. (left) Turbulent Energy Spectra against resolution scale for different models (ground-truth spectra in gray dashed line). (right) Ground-truth and reconstructed vector fields with proposed models.

network. A possible currently investigated solution is to consider different types of activation functions, such as sinusoidal functions as discussed in (Sitzmann et al., 2020).

When inspecting the Turbulent Kinetic Energy (TKE) spectra (see Figure 2), one can observe how the energy of high-frequency artifacts introduced by purely-data driven model is attenuated thanks to the self-similarity constraint. In particular, at the highest scales, corresponding to wavenumber $k > 10^2$, the curves of the TKE spectra featuring the self-similarity constraints are better aligned to the ground-truth ones. Nevertheless, the difference in height indicates that a lot of noise is still introduced by the models, suggesting that there is still room ror improvement.

5. Conclusions

This study proposed a physical-informed neural network to reconstruct an instantaneous 2D velocity field from sparse observation. Based on Multi-Layer-Perceptron and Random Fourier Fea-

tures, it takes as input any coordinates and outputs the associated velocity. Thanks to original physically-based regularization terms designed on higher spatial grids and exploiting automatic differentiation of neural networks, the proposed approach outperform standard methods, such as bi-cubic interpolation. It can be incorporated in other methods, for instance, extending the model operating on dynamic settings. In contrast with state-of-the-art models for super-resolution that typically process image-like data and require high-resolution labelled data, the proposed approach can process sparse grid-free observations in an unsupervised fashion. Numerical experimentation on synthetic data shows that the proposed approach can accurately reconstruct dense Eulerian velocity fields from sparse Lagrangian velocity measurements.

5.1. Broader Impact

In many domains spanning from geoscience to computer vision, from experimental fluid dynamics and medicine to art analysis, images can be modelled as the realization of vector fields transporting particles. Striking examples are satellites images of clouds, simulation of smokes, analysis of blood flows as well as the movement of the brush in a painting. Many related challenging tasks require to access such data at different resolution scales. PDEs can model the dynamics of such data with possibly complex boundary conditions, however standard solver suffers from computational issues due to the complexity of the problem. Moreover, these data often support sparse local measurements recorded by field sensors scattered on a broad area, for which grid-free approaches are desirable.
The proposed work gets in line with the physics-informed deep learning methods that, thanks to deep learning models' modularity and the possibility of easily encoding physics-based prior knowledge, try to address the known limitation of standard solvers. In particular, the proposed approach shows the possibility of reconstructing a high-resolution vector field while maintaining physical consistency and processing grid-free data.

References

Bar-Sinai, Y., Hoyer, S., Hickey, J., & Brenner, M. P. (2019). Learning data-driven discretizations for partial differential equations. *Proceedings of the National Academy of Sciences*, *116*(31), 15344–15349.

Beucler, T., Pritchard, M., Rasp, S., Ott, J., Baldi, P., & Gentine, P. (2021). Enforcing analytic constraints in neural networks emulating physical systems. *Physical Review Letters*, *126*(9), 098302.

Bode, M., Gauding, M., Lian, Z., Denker, D., Davidovic, M., Kleinheinz, K., … Pitsch, H. (2021). Using physics-informed enhanced super-resolution generative adversarial networks for subfilter modeling in turbulent reactive flows. *Proceedings of the Combustion Institute*, *38*(2), 2617–2625.

Bottero, L., Calisto, F., Graziano, G., Pagliarino, V., Scauda, M., Tiengo, S., & Azeglio, S. (2020). Physics-informed machine learning simulator for wildfire propagation. *arXiv preprint arXiv:2012.06825*.

Busch, J., Giese, D., Wissmann, L., & Kozerke, S. (2013). Reconstruction of divergence-free velocity fields from cine 3d phase-contrast flow measurements. *Magnetic resonance in medicine*, *69*(1), 200–210.

Cai, S., Zhou, S., Xu, C., & Gao, Q. (2019). Dense motion estimation of particle images via a convolutional neural network. *Experiments in Fluids*, *60*(4), 1–16.

Callaham, J., Maeda, K., & Brunton, S. L. (2018). Robust flow field reconstruction from limited measurements via sparse representation. *arXiv preprint arXiv:1810.06723*.

Deriaz, E., & Perrier, V. (2006). Divergence-free and curl-free wavelets in two dimensions and three dimensions: application to turbulent flows. *Journal of Turbulence*, *3*(7), N3.

Effinger, H., & Grossmann, S. (1987). Static structure function of turbulent flow from the navier-stokes equations. *Zeitschrift für Physik B Condensed Matter*, *66*(3), 289–304.

Esmaeilzadeh, S., Azizzadenesheli, K., Kashinath, K., Mustafa, M., Tchelepi, H. A., Marcus, P., … others (2020). Meshfreeflownet: a physics-constrained deep continuous space-time super-resolution framework. In *Sc20: International conference for high performance computing, networking, storage and analysis* (pp. 1–15).

Fukami, K., Fukagata, K., & Taira, K. (2019). Super-resolution reconstruction of turbulent flows with machine learning. *Journal of Fluid Mechanics*, *870*, 106–120.

Gao, H., Sun, L., & Wang, J.-X. (2021). Super-resolution and denoising of fluid flow using physics-informed convolutional neural networks without high-resolution labels. *Physics of Fluids*, *33*(7), 073603.

Gunes, H., & Rist, U. (2007). Spatial resolution enhancement/smoothing of stereo–particle-image-velocimetry data using proper-orthogonal-decomposition–based and kriging interpolation methods. *Physics of Fluids*, *19*(6), 064101.

Héas, P., Mémin, E., Heitz, D., & Mininni, P. D. (2012). Power laws and inverse motion modelling: application to turbulence measurements from satellite images. *Tellus A: Dynamic Meteorology and Oceanography*, *64*(1), 10962.

Hendriks, J., Jidling, C., Wills, A., & Schön, T. (2020). Linearly constrained neural networks. *arXiv preprint arXiv:2002.01600*.

Jacot, A., Gabriel, F., & Hongler, C. (2018). Neural tangent kernel: Convergence and generalization in neural networks. In S. Bengio, H. Wallach, H. Larochelle, K. Grauman, N. Cesa-Bianchi, & R. Garnett (Eds.), *Advances in neural information processing systems* (Vol. 31). Curran Associates, Inc. Retrieved from `https://proceedings.neurips.cc/paper/2018/file/5a4be1fa34e62bb8a6ec6b91d2462f5a-Paper.pdf`

Jin, X., Cai, S., Li, H., & Karniadakis, G. E. (2021). Nsfnets (navier-stokes flow nets): Physics-informed neural networks for the incompressible navier-stokes equations. *Journal of Computational Physics*, *426*, 109951.

Kashinath, K., Mustafa, M., Albert, A., Wu, J., Jiang, C., Esmaeilzadeh, S., ... others (2021). Physics-informed machine learning: case studies for weather and climate modelling. *Philosophical Transactions of the Royal Society A*, *379*(2194), 20200093.

Keys, R. (1981). Cubic convolution interpolation for digital image processing. *IEEE transactions on acoustics, speech, and signal processing*, *29*(6), 1153–1160.

Kim, B., Azevedo, V. C., Thuerey, N., Kim, T., Gross, M., & Solenthaler, B. (2019). Deep fluids: A generative network for parameterized fluid simulations. *Computer Graphics Forum*, *38*(2), 59–70.

Kim, H., Kim, J., Won, S., & Lee, C. (2021). Unsupervised deep learning for super-resolution reconstruction of turbulence. *Journal of Fluid Mechanics*, *910*.

Kim, T., Thürey, N., James, D., & Gross, M. (2008). Wavelet turbulence for fluid simulation. *ACM Transactions on Graphics (TOG)*, *27*(3), 1–6.

Kochkov, D., Smith, J. A., Alieva, A., Wang, Q., Brenner, M. P., & Hoyer, S. (2021). Machine learning–accelerated computational fluid dynamics. *Proceedings of the National Academy of Sciences*, *118*(21).

Lee, Y., Yang, H., & Yin, Z. (2017). Piv-dcnn: cascaded deep convolutional neural networks for particle image velocimetry. *Experiments in Fluids*, *58*(12), 171.

Li, Z., Kovachki, N., Azizzadenesheli, K., Liu, B., Bhattacharya, K., Stuart, A., & Anandkumar, A. (2020). Fourier neural operator for parametric partial differential equations. *arXiv preprint arXiv:2010.08895*.

Lu, L., Pestourie, R., Yao, W., Wang, Z., Verdugo, F., & Johnson, S. G. (2021). Physics-informed neural networks with hard constraints for inverse design. *arXiv preprint arXiv:2102.04626*.

Macêdo, I., & Castro, R. (2010). *Learning divergence-free and curl-free vector fields with matrix-valued kernels* (Tech. Rep.). Brasil, Tech. Rep.

McNally, C. P. (2011). Divergence-free interpolation of vector fields from point values - exact $\nabla \cdot \mathrm{B} = 0$ in numerical simulations. *Monthly Notices of the Royal Astronomical Society: Letters*, *413*(1), L76–L80.

Mohan, A. T., Lubbers, N., Livescu, D., & Chertkov, M. (2020). Embedding hard physical constraints in neural network coarse-graining of 3d turbulence. *arXiv preprint arXiv:2002.00021*.

Raissi, M., Perdikaris, P., & Karniadakis, G. E. (2019). Physics-informed neural networks: A deep learning framework for solving forward and inverse problems involving nonlinear partial differential equations. *Journal of Computational Physics*, *378*, 686–707.

Sitzmann, V., Martel, J., Bergman, A., Lindell, D., & Wetzstein, G. (2020). Implicit neural representations with periodic activation functions. *Advances in Neural Information Processing Systems*, *33*, 7462–7473.

Tancik, M., Srinivasan, P. P., Mildenhall, B., Fridovich-Keil, S., Raghavan, N., Singhal, U., ... Ng, R. (2020). Fourier features let networks learn high frequency functions in low dimensional domains. *arXiv preprint arXiv:2006.10739*.

Vinuesa, R., & Brunton, S. L. (2021). The potential of machine learning to enhance computational fluid dynamics. *arXiv preprint arXiv:2110.02085*.

Wang, C., Bentivegna, E., Zhou, W., Klein, L., & Elmegreen, B. (2020). Physics-informed neural network super resolution for advection-diffusion models. *arXiv preprint arXiv:2011.02519*.

Wang, R., Kashinath, K., Mustafa, M., Albert, A., & Yu, R. (2020). Towards physics-informed deep learning for turbulent flow prediction. In *Proceedings of the 26th acm sigkdd international conference on knowledge discovery & data mining* (pp. 1457–1466).

Wang, S., Wang, H., & Perdikaris, P. (2021). On the eigenvector bias of fourier feature networks: From regression to solving multi-scale pdes with physics-informed neural networks. *Computer Methods in Applied Mechanics and Engineering*, *384*, 113938.

Yang, J., Wright, J., Huang, T. S., & Ma, Y. (2010). Image super-resolution via sparse representation. *IEEE transactions on image processing*, *19*(11), 2861–2873.

Zille, P., Corpetti, T., Shao, L., & Xu, C. (2016). Super-resolution of turbulent passive scalar images using data assimilation. *Experiments in Fluids*, *57*(2), 21.